

A new class of exponential integrators for SDEs with multiplicative noise

UTKU ERDOĞAN

Nesin Mathematics Village, Şirince-Selçuk-Izmir 35920, Turkey

AND

GABRIEL J. LORD*

Department of Mathematics and Maxwell Institute for Mathematical Sciences,
Heriot Watt University, EH14 4AS Edinburgh, UK

*Corresponding author: g.j.lord@hw.ac.uk

[Received on 18 October 2016; revised on 16 January 2018]

In this paper, we present new types of exponential integrators for Stochastic Differential Equations (SDEs) that take advantage of the exact solution of (generalized) geometric Brownian motion. We examine both Euler and Milstein versions of the scheme and prove strong convergence, taking care to deal with the dependence on the noise in the solution operator. For the special case of linear noise we obtain an improved rate of convergence for the Euler version over standard integration methods. We investigate the efficiency of the methods compared with other exponential integrators for low dimensional SDEs and high dimensional SDEs arising from the discretization of stochastic partial differential equations. We show that, by introducing a suitable homotopy parameter, these schemes are competitive not only when the noise is linear, but also in the presence of nonlinear noise terms. Although our new schemes are derived and analysed under zero commutator conditions (1.2), our numerical investigations illustrate that the resulting methods rival traditional methods even when this does not hold.

Keywords: SDEs; exponential integrator; Euler Maruyama; exponential Milstein; homotopy; geometric Brownian motion.

1. Introduction

We develop new exponential integrators for the numerical approximation of stochastic differential equations (SDEs) of the following form:

$$d\mathbf{u} = (A\mathbf{u} + \mathbf{F}(\mathbf{u})) dt + \sum_{i=1}^m (B_i \mathbf{u} + \mathbf{g}_i(\mathbf{u})) dW_i(t), \quad \mathbf{u}(0) = \mathbf{u}_0 \in \mathbb{R}^d, \quad m, d \in \mathbb{N}, \quad (1.1)$$

where $W_i(t)$ are i.i.d. Brownian motions, $\mathbf{F}, \mathbf{g}_i : \mathbb{R}^d \rightarrow \mathbb{R}^d$, and the matrices $A, B_i \in \mathbb{R}^{d \times d}$, satisfy the following zero commutator conditions:

$$[A, B_i] = 0, \quad [B_j, B_i] = 0, \quad \text{for } i, j = 1 \dots m. \quad (1.2)$$

There are many SDE systems that can be written in this form, for example two well-known SDE systems are the FitzHugh–Nagumo equation with multiplicative noise (Hasegawa, 2008) and the Lotka–Volterra system (Li *et al.*, 2009). In practice, this form of SDEs is also encountered after space discretization

of stochastic partial differential equations (SPDEs) with diagonal noise (see Section 4.2). We derive our schemes and prove convergence under the condition (1.2). On the other hand, we see below that our schemes remain consistent and are efficient even for noncommutative matrices (see Section 4.3 and Section 4.4). In the deterministic setting, exponential integrators have proved to be very efficient for the numerical solution of stiff (partial) differential equations when compared to implicit solvers, see, for example, the review in the study by Hochbruck & Ostermann (2010). The derivation and usage of exponential integrators in the stochastic setting are still an active research area. Local linearization methods were first proposed by Biscay *et al.* (1996) and Jimenez *et al.* (1999) for SDEs with both additive and multiplicative noise. These methods continue to receive attention, for example Jimenez & Carbonell (2015) and Mora (2005) examine weak approximation and Carbonell & Jimenez (2008) consider more general noise terms. Recently Komori & Burrage (2014) examined mean square stability of exponential integrators for semilinear stiff SDEs. The method is the same basic one as developed for the space discretizations of SPDEs. For SPDEs with additive noise, Lord & Rougemont (2004) introduced an exponential scheme for stochastic PDEs that was later improved upon in the studies by Jentzen & Kloeden (2009) and Kloeden *et al.* (2011). Jentzen and co-workers (see, e.g. Jentzen 2009, 2010; Jentzen & Kloeden, 2009 and references therein) have further extended these results to include more general nonlinearities. There has been less work on exponential integrators with multiplicative noise. Strong convergence of stochastic exponential integrators for SDEs arising from the space discretization of SPDEs by a finite element method is considered in the study by Lord & Tambue (2012). More recently, a higher order exponential integrator of Milstein type was introduced in the study by Jentzen & Röckner (2015).

All the above exponential integrators for SDEs (e.g. arising from the discretization of the SPDEs) are based on the semigroup operator $\mathbf{S}_{t,t_0} = \exp((t-t_0)A)$ obtained from the following linear equation:

$$d\mathbf{S}_{t,t_0} = A\mathbf{S}_{t,t_0}dt, \quad \mathbf{S}_{t_0,t_0} = I_d,$$

where I_d is the unit matrix in $\mathbb{R}^{d \times d}$. For comparison, consider the following two standard exponential integrators for (1.1) with multiplicative noise: *SETD0*

$$\mathbf{u}_{n+1} = e^{\Delta t A} \left(\mathbf{u}_n + \mathbf{F}(\mathbf{u}_n) \Delta t + \sum_{i=1}^m (B_i \mathbf{u}_n + \mathbf{g}_i(\mathbf{u}_n)) \Delta W_{i,n} \right) \quad (1.3)$$

and *SETD1*

$$\mathbf{u}_{n+1} = e^{\Delta t A} \left(\mathbf{u}_n + \sum_{i=1}^m (B_i \mathbf{u}_n + \mathbf{g}_i(\mathbf{u}_n)) \Delta W_{i,n} \right) + \varphi(\Delta t A) \mathbf{F}(\mathbf{u}_n) \Delta t, \quad (1.4)$$

where

$$\varphi(A) = A^{-1} (\exp(A) - I_d), \quad \Delta t = t_{n+1} - t_n \quad \text{and} \quad \Delta W_{i,n} = W_i(t_{n+1}) - W_i(t_n).$$

These methods are essentially exact for a linear system of ODEs. We extend this approach to take advantage of the known solution of geometric Brownian motion in the numerical approximation. To do

this, we consider the linear homogeneous matrix differential equation

$$d\Phi_{t,t_0} = A\Phi_{t,t_0}dt + \sum_{i=1}^m B_i\Phi_{t,t_0}dW_i(t), \quad \Phi_{t_0,t_0} = I_d \quad (1.5)$$

and construct new schemes that are exact for a class of linear multiplicative SDEs of this form.

In the next section we derive our new exponential integrators for multiplicative noise and introduce the homotopy scheme. The main results of strong convergence analysis for the Euler and Milstein versions of the scheme are stated in Section 3 and for linear noise we obtain a strong rate of $\mathcal{O}(\Delta t)$ convergence for our Euler type scheme, improving over standard methods in this case. In addition we comment on mean-square stability in this section. Numerical examples are presented to examine the efficiency of the proposed schemes. We consider an SDE and a discretized SPDE where the commutator conditions (1.2) hold before looking at SDEs and a discretized SPDE where they do not. We see that in all the cases examined that the new schemes are competitive. Section 5 contains the proofs of strong convergence of $\mathcal{O}(\Delta t^{1/2})$ for the Euler version and $\mathcal{O}(\Delta t)$ for the Milstein version of our methods, and finally we conclude.

2. Derivation of the methods

Throughout we assume that $T \in (0, \infty)$ is a fixed real number and we have a partition of the time interval $[0, T]$, $0 = t_0 < t_1 < t_2 < \dots < t_N = T$ with constant step size $\Delta t = t_{j+1} - t_j$. Let $(\Omega, \mathcal{F}, \mathbb{P})$ be a probability space with filtration $(\mathcal{F}_t)_{t \in [0, T]}$. Then under suitable assumptions on \mathbf{F} and \mathbf{g}_i it is well known that there exists an \mathcal{F}_t -adapted stochastic process $u : [0, T] \times \Omega \rightarrow \mathbb{R}^d$ satisfying (1.1), (Mao, 1997; Øksendal, 2003; Lord *et al.*, 2014). The linear homogeneous matrix differential equation (1.5) has the exact solution

$$\Phi_{t,t_0} = \exp \left(\left(A - \frac{1}{2} \sum_{i=1}^m B_i^2 \right) (t - t_0) + \sum_{i=1}^m B_i (W_i(t) - W_i(t_0)) \right).$$

Let $\mathbf{u}(t)$ be the solution of (1.1) and take $t = t_{n+1}$, $t_0 = t_n$. Then, applying the Ito formula to $\mathbf{Y}(t) = \Phi_{t,t_0}^{-1}\mathbf{u}$, we obtain

$$\mathbf{u}(t_{n+1}) = \Phi_{t_{n+1},t_n} \left(\mathbf{u}(t_n) + \int_{t_n}^{t_{n+1}} \Phi_{s,t_n}^{-1} \tilde{\mathbf{f}}(\mathbf{u}(s)) 0 ds + \sum_{i=1}^m \int_{t_n}^{t_{n+1}} \Phi_{s,t_n}^{-1} \mathbf{g}_i(\mathbf{u}(s)) dW_i(s) \right), \quad (2.1)$$

where

$$\tilde{\mathbf{f}}(.) = \mathbf{F}(.) - \sum_{i=1}^m B_i \mathbf{g}_i(.). \quad (2.2)$$

Different treatment of the integrals in (2.1) leads to different numerical schemes. We examine Euler and Milstein type methods here, although clearly higher order methods, such as Wagner–Platen type schemes (see for example Becker *et al.*, 2016), could be developed. Derivation of the methods below

uses the commutativity of the matrices in (1.2). This condition does not hold in general. However, it is straightforward to show by an Ito–Taylor expansion consistency of the methods for the noncommutative case. Numerically we observe that the accompanying error is small (see Section 4.3 and Section 4.4). First we derive Euler type Exponential Integrators and then in Section 2.2 turn to Milstein versions.

2.1 Euler type Exponential Integrators

We take the following approximation for the stochastic integral in (2.1):

$$\Phi_{t_{n+1}, t_n} \int_{t_n}^{t_{n+1}} \Phi_{s, t_n}^{-1} \mathbf{g}_i(\mathbf{u}(s)) dW_i(s) \approx \Phi_{t_{n+1}, t_n} \mathbf{g}_i(\mathbf{u}(t_n)) \Delta W_{i,n}, \quad (2.3)$$

where $\Delta W_{i,n} = W_i(t_{n+1}) - W_i(t_n)$ and we derive Euler type Exponential Integrators below. For the deterministic integral in (2.1) we examine three cases.

1. Taking $\Phi_{t_{n+1}, t_n} \int_{t_n}^{t_{n+1}} \Phi_{s, t_n}^{-1} \tilde{\mathbf{f}}(\mathbf{u}(s)) ds \approx \Phi_{t_{n+1}, t_n} \tilde{\mathbf{f}}(\mathbf{u}(t_n)) \Delta t$, we obtain our first method *EI0*

$$\mathbf{u}_{n+1} = \Phi_{t_{n+1}, t_n} \left(\mathbf{u}_n + \tilde{\mathbf{f}}(\mathbf{u}_n) \Delta t + \sum_{i=1}^m \mathbf{g}_i(\mathbf{u}_n) \Delta W_{i,n} \right).$$

2. If we take $\Phi_{t_{n+1}, s} \int_{t_n}^{t_{n+1}} \Phi_{s, t_n}^{-1} \tilde{\mathbf{f}}(\mathbf{u}(s)) ds \approx \mathbf{Z}_{t_{n+1}, t_n} \varphi(\Delta t A) \tilde{\mathbf{f}}(\mathbf{u}(t_n)) \Delta t$ where

$$\mathbf{Z}_{t,s} = \exp \left(-\frac{1}{2} \sum_{i=1}^m B_i^2(t-s) + \sum_{i=1}^m B_i (W_i(t) - W_i(s)) \right)$$

then we obtain our second method *EI1*

$$\mathbf{u}_{n+1} = \Phi_{t_{n+1}, t_n} \left(\mathbf{u}_n + \sum_{i=1}^m \mathbf{g}_i(\mathbf{u}_n) \Delta W_{i,n} \right) + \mathbf{Z}_{t_{n+1}, t_n} \varphi(\Delta t A) \tilde{\mathbf{f}}(\mathbf{u}_n) \Delta t.$$

3. Finally with $\Phi_{t_{n+1}, t_k} \int_{t_n}^{t_{n+1}} \Phi_{s, t_n}^{-1} \tilde{\mathbf{f}}(\mathbf{u}(s)) ds \approx \varphi(\Delta t A) \tilde{\mathbf{f}}(\mathbf{u}(t_n)) \Delta t$, we get the method *EI2*

$$\mathbf{u}_{n+1} = \Phi_{t_{n+1}, t_n} \left(\mathbf{u}_n + \sum_{i=1}^m \mathbf{g}_i(\mathbf{u}_n) \Delta W_{i,n} \right) + \varphi(\Delta t A) \tilde{\mathbf{f}}(\mathbf{u}_n) \Delta t.$$

We focus on *EI0*, however we compare the accuracy and efficiency of these approximations in Section 4. For general noise the schemes *EI0*, *EI1*, *EI2* all have the same strong rate of convergence as *SETD0* in (1.3) and *SETD1* (1.4) which is $\mathcal{O}(\Delta t^{1/2})$. However, we expect an improvement in the error when the terms in B_i dominate \mathbf{g}_i in the noise. In the special case where $\mathbf{g}_i \equiv 0$ we prove, and show numerically, an improvement in the strong rate of convergence to $\mathcal{O}(\Delta t)$.

It should be noted that all the proposed new type integrators reduce to the usual exponential integrators *SETD0* and *SETD1* when $B_i = 0$, $i = 1 \dots m$. Indeed, it is observed in numerical simulations that *SETD* schemes may perform better than the new *EI* schemes when the B_i are small compared to \mathbf{g}_i . On the other hand the *EI* schemes outperform *SETD* schemes when B_i are dominant. We can capture

the good properties of both methods by introducing a homotopy parameter $p \in [0, 1]$. Let us rewrite (1.1) as

$$d\mathbf{u} = (A\mathbf{u} + \mathbf{F}(\mathbf{u})) dt + \sum_{i=1}^m (pB_i\mathbf{u} + [\mathbf{g}_i(\mathbf{u}) + (1-p)B_i\mathbf{u}]) dW_i(t). \quad (2.4)$$

For example, applying *EIO* for this equation, one obtains *HomEIO*

$$\mathbf{u}_{n+1} = \Phi_{t_{n+1}, t_n}^p \left(\mathbf{u}_n + \tilde{\mathbf{f}}^p(\mathbf{u}_n) \Delta t + \sum_{i=1}^m \mathbf{g}_i^p(\mathbf{u}_n) \Delta W_{i,n} \right), \quad (2.5)$$

where

$$\Phi_{t_{n+1}, t_n}^p = \exp \left(\left(A - \frac{1}{2} \sum_{i=1}^m p^2 B_i^2 \right) \Delta t + \sum_{i=1}^m p B_i \Delta W_{i,n} \right), \quad (2.6)$$

$$\mathbf{g}_i^p(\mathbf{u}) = \mathbf{g}_i(\mathbf{u}) + (1-p)B_i\mathbf{u}, \quad \text{and} \quad \tilde{\mathbf{f}}^p(\mathbf{u}) = \mathbf{F}(\mathbf{u}) - \sum_{i=1}^m p B_i \mathbf{g}_i^p(\mathbf{u}). \quad (2.7)$$

It is clear that $p = 0$ and $p = 1$ give *SETD0* and *EIO*, respectively. In Section 4 we suggest a fixed formula for p based on the weighting of B_i to \mathbf{g}_i (see (4.2)). However, further consideration could be given to an optimal choice of either a fixed p or of a p assigned during the computation by considering weights of the terms in the diffusion coefficient, so that $p(u, B_i, g_i)$. We note that unlike Milstein methods, *HomEIO* and the other *EI* methods have the advantage that they do not require the derivative of the diffusion term.

2.2 Milstein type Exponential Integrators

An alternative treatment of (2.1) is to use the Ito–Taylor expansion of the diffusion term

$$\Phi_{s, t_n}^{-1} \mathbf{g}_i(\mathbf{u}(s)) = \mathbf{g}_i(\mathbf{u}(t_n)) + \sum_{l=1}^m \int_{t_n}^s \Phi_{r, t_n}^{-1} \mathbf{H}_{i,l}(\mathbf{u}(r)) dW_l(r) + \int_{t_n}^s \Phi_{r, t_n}^{-1} \mathbf{Q}_i(\mathbf{u}(r)) dr, \quad (2.8)$$

where

$$\mathbf{H}_{i,l}(\mathbf{u}(.)) = D\mathbf{g}_i(\mathbf{u}(.)) (B_l \mathbf{u}(.)) + \mathbf{g}_l(\mathbf{u}(.)) - B_l \mathbf{g}_i(\mathbf{u}(.)) \quad (2.9)$$

and $\mathbf{Q}_i(.)$ is the vector function in terms of A , \mathbf{F} , $D\mathbf{g}_i$, $D^2\mathbf{g}_i$, B_l for $i, l = 1, \dots, m$ (which, for ease of presentation, we do not detail here).

Freezing the integrand of stochastic integral at $r = t_n$ and dropping the deterministic integral

$$\Phi_{s, t_n}^{-1} \mathbf{g}_i(\mathbf{u}(s)) = \mathbf{g}_i(\mathbf{u}(t_n)) + \sum_{l=1}^m \int_{t_n}^s \mathbf{H}_{i,l}(\mathbf{u}(t_n)) dW_l(r) + h.o.t. \quad (2.10)$$

then dropping the higher order terms, we obtain the Milstein scheme *MI0*

$$\mathbf{u}_{n+1} = \Phi_{t_{n+1}, t_n} \left(\mathbf{u}_n + \tilde{\mathbf{f}}(\mathbf{u}_n) \Delta t + \sum_{i=1}^m \mathbf{g}_i(\mathbf{u}_n) \Delta W_{i,n} + \sum_{i=1}^m \sum_{l=1}^m \mathbf{H}_{i,l}(\mathbf{u}_n) \int_{t_n}^{t_{n+1}} \int_{t_n}^s dW_l(r) dW_i(s) \right), \quad (2.11)$$

where $\tilde{\mathbf{f}}$ is defined as in (2.2). We also introduce a Milstein homotopy type scheme *HomMIO* by applying *MIO* to (2.4).

3. Strong convergence and mean-square stability

We state in this section the strong convergence result for both *EIO* and *MIO*. Proofs are given in Section 5 and we note that the proofs for the other schemes, including those such as (2.5), are similar. For these proofs we assume a global Lipschitz condition on the drift and diffusion although tamed versions of the methods for more general drift and diffusions can be derived. We let $\|\cdot\|_2$ denote the standard Euclidean norm for both vectors and matrices and $\|\cdot\|_{L^2(\Omega, \mathbb{R}^d)}^2 = \mathbb{E}[\|\cdot\|_2^2]$.

ASSUMPTION 1 There exists a constant $L > 0$ such that the linear growth condition holds: for $\mathbf{u} \in \mathbb{R}^d$ and $i = 1, \dots, m$

$$\|\mathbf{F}(\mathbf{u})\|_2^2 \leq L(1 + \|\mathbf{u}\|_2^2), \quad \|\mathbf{g}_i(\mathbf{u})\|_2^2 \leq L(1 + \|\mathbf{u}\|_2^2),$$

and the global Lipschitz condition holds: for $\mathbf{u}, \mathbf{v} \in \mathbb{R}^d$, $i = 1, \dots, m$

$$\|\mathbf{F}(\mathbf{u}) - \mathbf{F}(\mathbf{v})\|_2 \leq L \|\mathbf{u} - \mathbf{v}\|_2, \quad \|\mathbf{g}_i(\mathbf{u}) - \mathbf{g}_i(\mathbf{v})\|_2 \leq L \|\mathbf{u} - \mathbf{v}\|_2.$$

First we state the strong convergence result for the Euler type scheme *EIO*.

THEOREM 3.1 Let Assumptions 1 hold and let \mathbf{u}_n be the approximation to the solution of (1.1) using *EIO*. Then, for $T > 0$, there exists $K > 0$ independent of Δt such that

$$\sup_{0 \leq t_n \leq T} \|\mathbf{u}(t_n) - \mathbf{u}_n\|_{L^2(\Omega, \mathbb{R}^d)} \leq K \Delta t^{1/2}. \quad (3.1)$$

For the Milstein scheme *MIO*, we impose the following two extra assumptions.

ASSUMPTION 2 The functions $F, \mathbf{g}_i : \mathbb{R}^d \rightarrow \mathbb{R}^d$ are twice continuously differentiable.

ASSUMPTION 3 For the same constant L as in Assumption 1 for $\mathbf{u}, \mathbf{v} \in \mathbb{R}^d$, $i, l = 1, \dots, m$

$$\|D\mathbf{g}_i(\mathbf{u})\mathbf{g}_l(\mathbf{u}) - D\mathbf{g}_i(\mathbf{v})\mathbf{g}_l(\mathbf{v})\|_2 \leq L \|\mathbf{u} - \mathbf{v}\|_2$$

and

$$\|D\mathbf{g}_i(\mathbf{u})B_l\mathbf{u} - D\mathbf{g}_i(\mathbf{v})B_l\mathbf{v}\|_2 \leq L \|\mathbf{u} - \mathbf{v}\|_2.$$

THEOREM 3.2 Let Assumptions 1, 2, and 3 hold and let \mathbf{u}_n be the approximation to the solution of (1.1) using *MIO*. Then, for $T > 0$, there exists $K > 0$ independent of Δt such that

$$\sup_{0 \leq t_n \leq T} \|\mathbf{u}(t_n) - \mathbf{u}_n\|_{L^2(\Omega, \mathbb{R}^d)} \leq K \Delta t. \quad (3.2)$$

Note that from the definition of $\tilde{\mathbf{f}}$ in (2.2) and $\mathbf{H}_{i,l}$ in (2.9), these functions also satisfy global Lipschitz and/or continuously differentiability conditions when the corresponding assumptions on \mathbf{F} , \mathbf{g}_i and $D\mathbf{g}_i$ hold. We give the proofs of Theorem 3.1 and Theorem 3.2 in Section 5.

Now consider the special case when $\mathbf{g}_i \equiv 0$ in (1.1). Namely, we have the SDE

$$d\mathbf{u} = (A\mathbf{u} + \mathbf{F}(\mathbf{u})) dt + \sum_{i=1}^m B_i \mathbf{u} dW_i(t), \quad \mathbf{u}(0) = \mathbf{u}_0 \in \mathbb{R}^d, \quad (3.3)$$

for which both the numerical schemes *EI0* and *MI0* reduce to

$$\mathbf{u}_n = \Phi_{t_{n+1}, t_n} (\mathbf{u}_n + \mathbf{F}(\mathbf{u}_n) \Delta t). \quad (3.4)$$

Remark that we can consider (3.4) as a Lie–Trotter splitting of (3.3). It is straightforward to conclude the following improvement in the convergence rate for *EI0*.

COROLLARY 1 Suppose that Assumption 1 holds and \mathbf{F} is continuously differentiable. Let \mathbf{u}_n denote the approximation to the solution of (3.3) by (3.4). Then for $T > 0$, there exists $K > 0$ independent of Δt such that

$$\sup_{0 \leq t_n \leq T} \|\mathbf{u}(t_n) - \mathbf{u}_n\|_{L^2(\Omega, \mathbb{R}^d)} \leq K \Delta t. \quad (3.5)$$

This is a simple consequence of solving the linear SDE exactly, see Section 5.

3.1 Mean-Square stability of *HomEI0*

The standard one-dimensional SDE used to examine mean square stability is given by

$$du = \lambda u dt + \mu u dW, \quad u(0) = u_0 \in \mathbb{R}, \quad (3.6)$$

where λ and μ are allowed to be complex, see for example the studies by Buckwar & Kelly (2010), Komori & Burrage (2014) and Saito & Mitsui (1996). Assuming $u_0 \neq 0$, then the exact solution $u(t)$ of (3.6) satisfies

$$\lim_{t \rightarrow \infty} \mathbb{E}|u(t)|^2 = 0 \quad \text{if and only if} \quad \mathcal{R}\{\lambda\} + \frac{1}{2}|\mu|^2 < 0.$$

The proposed method *EI0* exactly solves (3.6) and its stability region is given by

$$\hat{R}_{EI0} = \left\{ (z_1, z_2) \mid z_1 + \frac{1}{2}z_2 < 0 \right\},$$

where $z_1 = \mathcal{R}(\lambda)\Delta t$ and $z_2 = |\mu|^2\Delta t$. To determine the stability region of *HomEI0* method, we apply *EI0* to the test equation (3.6) in the following form:

$$du = \lambda u dt + (p\mu u + (1-p)\mu u) dW, \quad u(0) = u_0.$$

We obtain the stability region

$$\hat{R}_{HomEI0} = \left\{ (z_1, z_2) \mid e^{2z_1 + p^2 z_2} \left(1 + z_2(1-p^2) + z_2^2 p^2 (p-1)^2 \right) < 1 \right\},$$

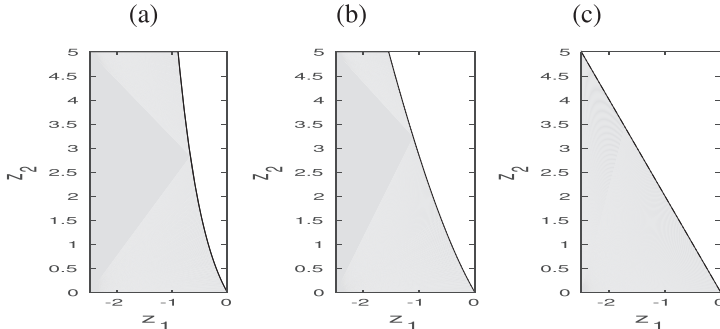


FIG. 1. Mean-square stability regions for *HomEIO* with (a) $p = 0$ (*SETD0*), (b) $p = 1/2$ and (c) $p = 1$ (*EI0*).

where the cases $p = 0$ and $p = 1$ correspond to *SETD0* and *EI0*, respectively. Therefore, the stability region of *HomEIO* shrinks continuously as p changes from 0 to 1 and $\hat{R}_{\text{EI0}} \subset \hat{R}_{\text{HomEIO}} \subset \hat{R}_{\text{SETD0}}$. This is illustrated in Fig. 1.

4. Numerical examples

In this section we perform some numerical experiments to illustrate and confirm the orders of the proposed methods. For comparison *SETD0*, *SETD1*, Exponential Milstein *ExpMIL* (Jentzen & Röckner, 2015), the classical Milstein (Kloeden & Platen, 2011) are used as well as the semiimplicit Euler–Maruyama (EM) scheme. We consider SDEs of the form of (1.1) and in particular we introduce two parameters α and β so that we have

$$d\mathbf{u} = (A\mathbf{u} + \mathbf{F}(\mathbf{u})) dt + \sum_{i=1}^m (\beta B_i \mathbf{u} + \alpha \mathbf{g}_i(\mathbf{u})) dW_i(t), \quad \mathbf{u}(0) = \mathbf{u}_0 \in \mathbb{R}^d \quad m, d \in \mathbb{N}. \quad (4.1)$$

When $\alpha \ll \beta$ the linear terms B_i dominate, whereas if $\alpha \gg \beta$, the nonlinearity \mathbf{g}_i dominates. By examining different α and β we can see the effect of the strength of the nonlinearity.

For *HomEIO* and *HomMIO* we define the homotopy parameter by

$$p = \frac{|\beta|}{|\alpha| + |\beta|}. \quad (4.2)$$

Where we do not have an exact solution below we compute a reference solution using the exponential Milstein method with a small step size Δt_{ref} and examine a Monte Carlo estimate of $\|\mathbf{u}(t_n) - \mathbf{u}_n\|_{L^2(\Omega, \mathbb{R}^d)}$, the root mean square error (RMSE), with M realizations. In Section 4.1 and Section 4.2 the commutativity conditions (1.2) hold unlike our examples in Section 4.3 and Section 4.4.

4.1 The Ginzburg–Landau equation

Consider the one-dimensional equation

$$du(t) = \left(-u + \frac{\sigma}{2} u - u^3 \right) dt + \sqrt{\sigma} u dW(t), \quad u(0) = u_0 \quad (4.3)$$

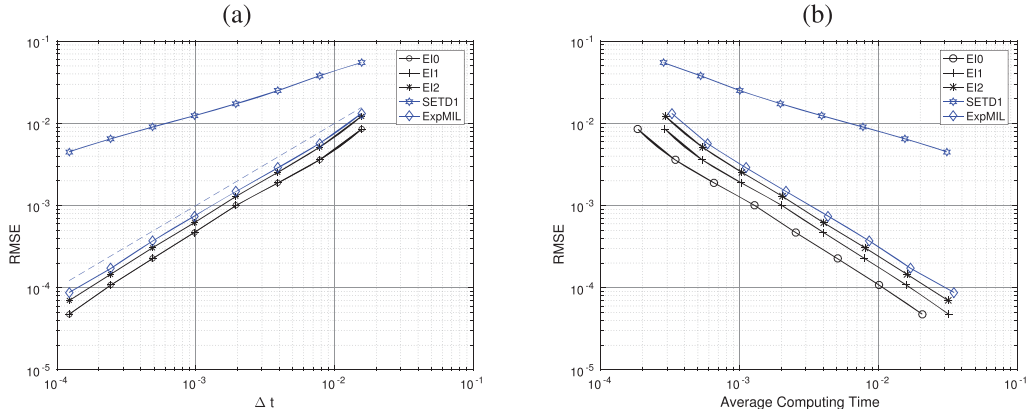


FIG. 2. Stochastic Ginzburg–Landau Equation (26) with $\sigma = 2$, $T = 1$, $M = 1000$ samples (a) RMSE against Δt . Also plotted is a reference line with slope 1. (b) RMSE against cpitime. Of the new schemes $EI0$ is the most efficient. We observe the improved convergence rate of Corollary 3.1 in these new schemes over that for $SETD1$.

that has exact solution (Kloeden & Platen, 2011)

$$u(t) = \frac{u_0 e^{-t+\sqrt{\sigma}W(t)}}{\sqrt{1 + 2u_0^2 \int_0^t e^{-2s+2\sqrt{\sigma}W(s)} ds}}. \quad (4.4)$$

It should be noted that the drift term satisfies only a one-sided global Lipschitz condition and our proposed schemes can be tamed to guarantee strong convergence as in the study by Hutzenthaler & Jentzen, 2015. Nevertheless, simulations reveal the performance of the new schemes $EI0$, $EI1$ and $EI2$ and act as a benchmark for $SETD1$ (see also Jentzen & Röckner, 2015). Note that (26) is linear in the diffusion and hence Corollary 3.1 holds, and we expect first order convergence, and MIO and $HomMIO$ both reduce to $EI0$ and $HomEI0$. This is observed numerically in Fig. 2(a) where we see first order convergence of the methods $EI0$, $EI1$ and $EI2$. In Fig. 2(b) we compare the efficiency of the schemes and observe that $EI0$ is the most efficient. From now on we no longer consider $EI1$ or $EI2$.

4.2 A spectral Galerkin discretization of an SPDE

We examine the strong convergence of the schemes $EI0$, $HomEI0$ applied to SDEs arising from the spectral Galerkin discretization in space of an SPDE. Consider the stochastic reaction–diffusion equation

$$du = \left[\varepsilon \frac{\partial^2 u}{\partial x^2} + 1 - u \right] dt + \left[\beta u + \alpha \frac{1-u}{1+u^2} \right] dW(t), \quad u(x, 0) = u_0(x) = \sin(\pi x), \quad (4.5)$$

with $x \in [0, 1]$ subject to zero Dirichlet boundary conditions. We take $W(t)$ to be a Q –Wiener process and let Q have orthonormal eigenfunctions $g_j(x) = \sqrt{2} \sin(j\pi x)$ and eigenvalues $v_j = \frac{1}{j^2}, j \in \mathbb{N}$, so that

$$W(t) = \sum_{j \in \mathbb{N}} \frac{1}{j} g_j \beta_j(t),$$

Algorithm 1 Script to solve (28) by using *EIO* combined with a spectral Galerkin method.

```

1 N=pow2(18);T=1.0;Dt=T/N; %number of steps,final time,step size
2 d=128;J=[1:d]'; %spatial discretization
3 A=-pi^2*J.^2/100; mu=J.^(-2); %linear operator and e.val for
%noise
4 y=sin(pi.*J/(d+1)); Y=idst(y)/sqrt(2); % initial data
5 beta=1;alpha=0.1; % problem parameters
6 b=@(x) alpha*(1-x)./(1+x.^2); % set functions
7 f=@(x) 1-x;
8 g=zeros(d,1);
9 for j=1:d
10 g=g+2*sin(j.*J./(d+1).*pi).^2.*mu(j);
11 end
12 for j=1:N % loop over time steps
13 y=dst(Y)*sqrt(2); % get discrete sine transform
14 dW=dst(randn(d,1).*sqrt(Dt.*mu.*2)); % get increment for noise
15 % update step
16 y=exp(-beta^2/2*g.*Dt+beta*dW).* ( y+(f(y)-beta.*g.*b(y))
    .*Dt+b(y).*dW);
17 Y=exp(Dt*A).*idst(y)/sqrt(2);
18 end

```

where $\beta_j(t)$ are i.i.d. Brownian motions. Applying the spectral Galerkin method as described for example in the study by Jentzen & Röckner (2015) to discretize in space, we implement *EIO* in Algorithm 1. In the notation of (1.1) for the SDEs after spatial discretization the commutator conditions (1.2) hold. We note that Jentzen and Röckner derived the special case of *EIO* for $\alpha = 0$ in Jentzen & Röckner (2015) as a splitting procedure. However, they employed exponential based schemes without computing exponentials of diffusion coefficients for nonzero α values. In Fig. 3 we show convergence (a) and efficiency (b) of the method *EIO* compared to EM and *SETDO* with $\beta = 1$ and $\alpha = 0$. By our choice of p in (4.2) with $\alpha = 0$ the scheme *HomEIO* reduces to *EIO*. In Fig. 4 we include nonlinearity and take $\alpha = 1$. The linear and nonlinear terms are equally weighted and we see that *HomEIO* is more efficient than the standard integrators.

4.3 Noncommutativity and nonlinear noise

Consider the following SDE in \mathbb{R}^4 , with initial data $\mathbf{u}(0) = (1, 1, 1, 1)^T$

$$d\mathbf{u} = (rA\mathbf{u} + \mathbf{F}(\mathbf{u})) dt + G(\mathbf{u})d\mathbf{W}(t), \quad F_j = \frac{u_j}{1 + |u_j|}, \quad (4.6)$$

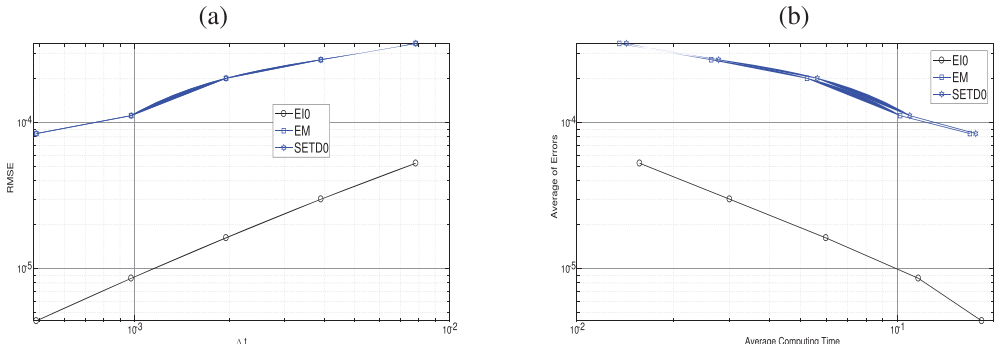


FIG. 3. Equation (4.5) with $\varepsilon = 0.01$, $T = 1$ and $M = 1000$ samples with $\beta = 1$, $\alpha = 0$, for which HomEI0 and $EI0$ are the same and the noise consists of a linear diagonal term. In (a) we show the RMSE against Δt , and in (b) RMSE against cputime. We observe that $EI0$ is the most efficient.

where r is a constant (we take $r = 4$) and A arises from the standard finite difference approximation of the Laplacian

$$A = \begin{pmatrix} -2 & 1 & 0 & 0 \\ 1 & -2 & 1 & 0 \\ 0 & 1 & -2 & 1 \\ 0 & 0 & 1 & -2 \end{pmatrix}. \quad (4.7)$$

For a general matrix B we have $[A, B] \neq 0$ and the commutator conditions (1.2) will not hold below. However, it is straightforward to show by an Ito–Taylor expansion consistency of the methods, and we show numerically below that the accompanying error is small.

Diagonal noise

First we look at diagonal noise and examine the affect of the noise being dominated by either linear or nonlinear terms. For the nonlinear part we let $g(u) = 1/(1 + u^2)$ and let $\mathbf{g}_i(\mathbf{u})$ have only one nonzero

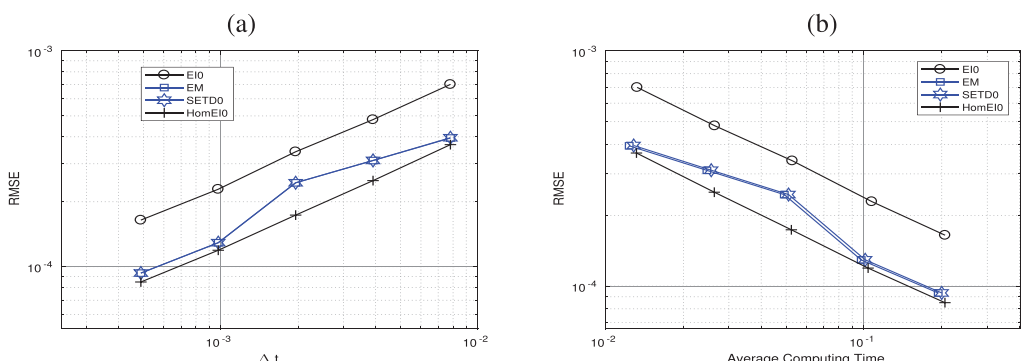


FIG. 4. Equation (4.5) with $\varepsilon = 0.01$, $T = 1$ and $M = 1000$ samples with $\beta = 1$, $\alpha = 1$. In (a) we show the RMSE against Δt , and in (b) the RMSE against cputime. We see that HomEI0 is the most efficient.

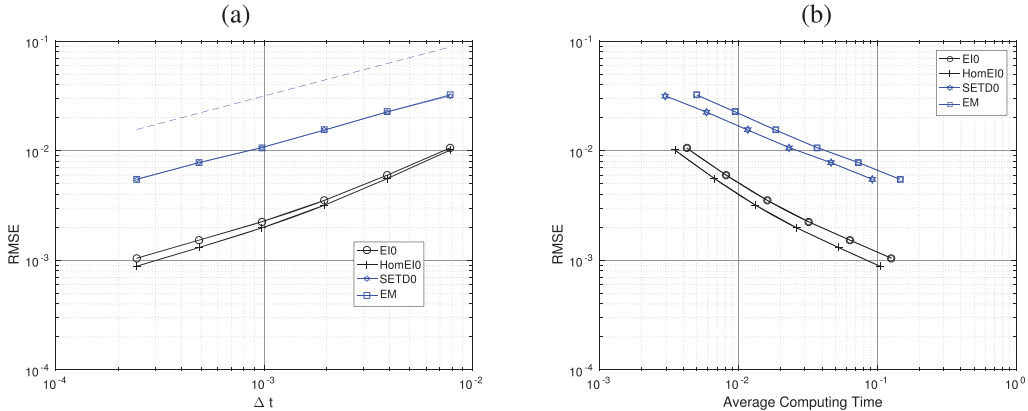


FIG. 5. Euler methods. Equation (4.6) $\beta = 1, \alpha = 0.1, r = 4, T = 1$ and $M = 1000$ samples (a) RMSE against Δt . Also plotted is a reference line with slope 1/2. (b) RMSE against cputime. Here the linear noise term dominates and we see *HomEIO* is the most efficient, followed by *EIO*. See Fig. 6 for Milstein schemes.

element $\alpha g(u_i)$ in the i th entry for $\alpha \in \mathbb{R}$. For the linear part we take $B_i = \beta \text{diag}(\mathbf{e}_i)$ where \mathbf{e}_i is the i th unit vector of \mathbb{R}^4 and $\beta \in \mathbb{R}$ and as noted above $[A, B_i] \neq 0$. This gives $G(u)$ in (4.6) as

$$G(\mathbf{u}) = \begin{pmatrix} \beta u_1 + \alpha g(u_1) & 0 & 0 & 0 \\ 0 & \beta u_2 + \alpha g(u_2) & 0 & 0 \\ 0 & 0 & \beta u_3 + \alpha g(u_3) & 0 \\ 0 & 0 & 0 & \beta u_4 + \alpha g(u_4) \end{pmatrix}.$$

A script to implement *HomEIO* is presented in Algorithm 2. We show results for both the Euler and Milstein type schemes for different α and β values with a reference step size $\Delta t_{\text{ref}} = 2^{-20}$.

Consider the case where $\alpha = 0.1$ and $\beta = 1$ so that the linear term dominates. Figure 5(a) illustrates orders and (b) the efficiency of the methods *EIO*, *SETD0*, *HomEIO*. In Fig. 5(a) we see convergence with the predicted rate and in Fig. 5(b) it is clear that *EIO* and *HomEIO* are more efficient than either *SETD0* or the semiimplicit *EM* method. Recall that if $\alpha = 0$ then we obtain first order convergence for *EIO* and *HomEIO*, which is not the case for *SETD0* or *EM*. Figure 6(a) shows first order convergence for the Milstein schemes, and from (b) we see that *HomMIO* and *MIO* are the most efficient.

However, when $\beta = \alpha = 1$ (and we have equal weighting between the linear and nonlinear term) we see in Fig. 7(a) the same rate of convergence, but now *HomEIO* is more accurate than *EIO*, and from Fig. 7(b) that *HomEIO* is still the most efficient, followed by *SETD0*. This illustrates the effectiveness of adding the homotopy parameter. For the Milstein schemes we see the predicted rate of convergence in Fig. 8(a), and in (b) that *HomEIO* and *MIO* are very marginally more efficient than either the classical Milstein or Exponential Milstein schemes.

In Fig. 9 we have $\beta = 0.1$ and $\alpha = 1$ so that it is the nonlinearity that dominates. We now see that the errors from *HomEIO* are similar to those of the standard integrators *SETD0* and *EM*, and that *SETD0* is now more efficient. We note, however, that *HomEIO* remains more efficient than *EM*. For the Milstein schemes we see the predicted rate of convergence in Fig. 10(a), and in (b) that *HomEIO* and *MIO* are more efficient than either the classical Milstein or Exponential Milstein schemes.

Algorithm 2 Script to solve (29) with noise given by (31) using *HomEIO*.

```

1 N=pow2(10);T=1.0;Dt=T/N;%number of steps,final time,step size
2 d=4;m=4;% dimension of problem and dimension of noise
3 r=4;beta=1;alpha=0.1;% parameters of the problem
4 X=ones(d,1);%initial Condition
5 p=abs(beta)/(abs(beta)+abs(alpha));%set homotopy parameter
6 % Set Matrices
7 A=-r*sparse(toeplitz([2 -1 zeros(1,d-2)])); M1=expm(Dt*A);
8 % Set functions
9 f=@(u) u./(1+abs(u)); g=@(u) 1./(1+u.^2);
10 ftild=@(u) f(u)-p*beta*(alpha*g(u)+(1-p)*beta*u);
11 Gtild=@(u) alpha*g(u)+(1-p)*beta*u;
12 for n=1:N % loop over time steps
13     dW = sqrt(Dt)*randn(m,1); % get increment for noise
14     M2 = exp(-Dt*0.5*p^2*beta^2+p*beta*dW);
15     X=M1*M2.* (X+Dt*ftild(X)+Gtild(X).*dW); % update step
16 end

```

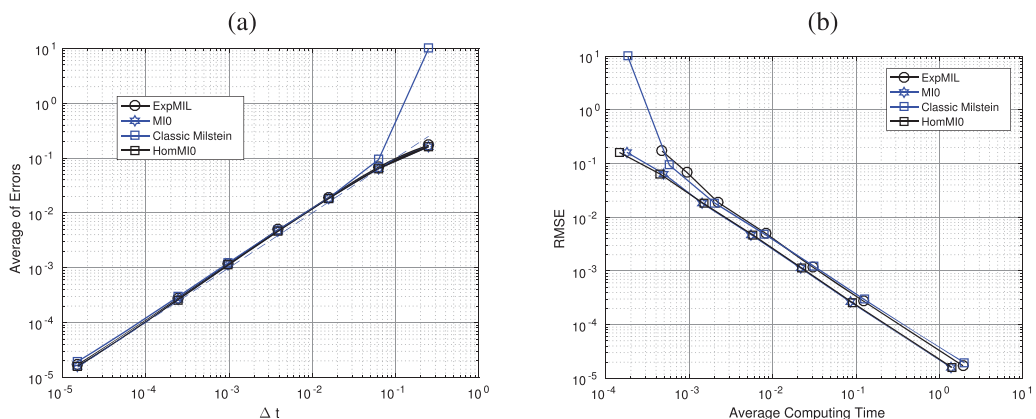


FIG. 6. Milstein methods. Equation (4.6) with $\beta = 1$, $\alpha = 0.1$, $r = 4$, $T = 1$ and $M = 100$ samples (a) RMSE against Δt . Also plotted is a reference line with slope 1 (compare to Fig. 5). In (b) RMSE against cputime. Here the linear noise term dominates and we see *HomMIO* and *MIO* are the most efficient.

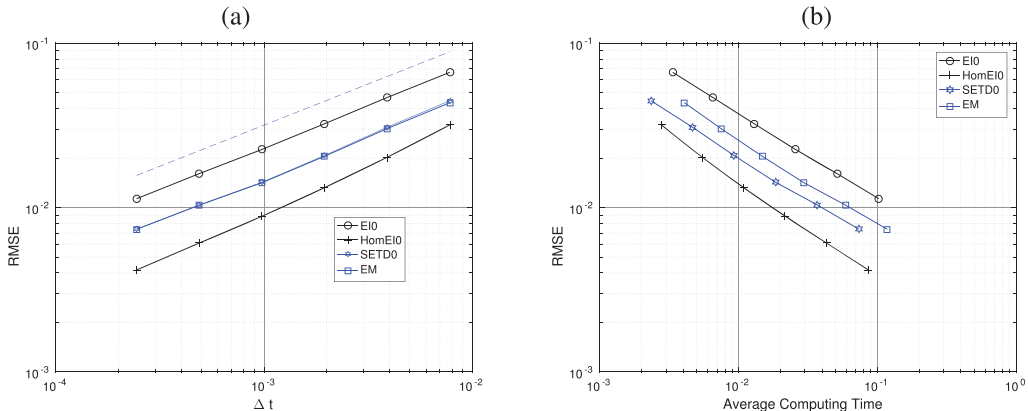


FIG. 7. Euler methods. Equation (4.6) with $\beta = 1$, $\alpha = 1$, $r = 4$, $T = 1$ and $M = 1000$ samples (a) RMSE against Δt . Also plotted is a reference line with slope 1/2. (b) RMSE against cputime. We have equal weighting of linear and nonlinear noise terms and we see *HomE10* is clearly the most efficient and accurate. See Fig. 8 for Milstein type schemes.

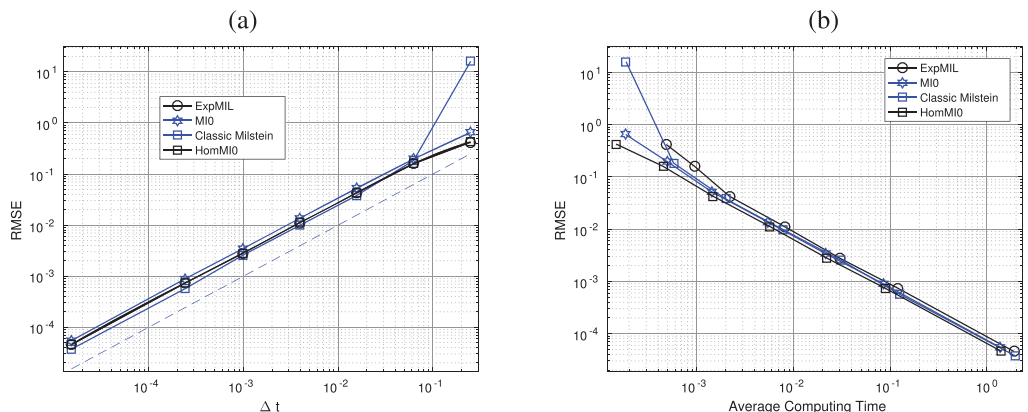


FIG. 8. Milstein methods. Equation (4.6) with $\beta = 1$, $\alpha = 1$, $r = 4$, $T = 1$ and $M = 100$ samples (a) root mean square error against Δt . Also plotted is a reference line with slope 1 (compare to Fig. 7). In (b) root mean square error against cputime. With equal weighting of the noise we see *HomM10* and *M10* are marginally more efficient.

Nondiagonal noise

Now consider (4.6) with noncommutative noise by taking the following diffusion coefficient matrix:

$$G(\mathbf{u}) = \begin{pmatrix} \beta u_1 & 0 & 0 & 0 \\ 0 & \beta u_2 - \alpha u_1 & 0 & 0 \\ 0 & 0 & \beta u_3 - \alpha u_2 & 0 \\ 0 & 0 & 0 & \beta u_4 - \alpha u_3 \end{pmatrix}. \quad (4.8)$$

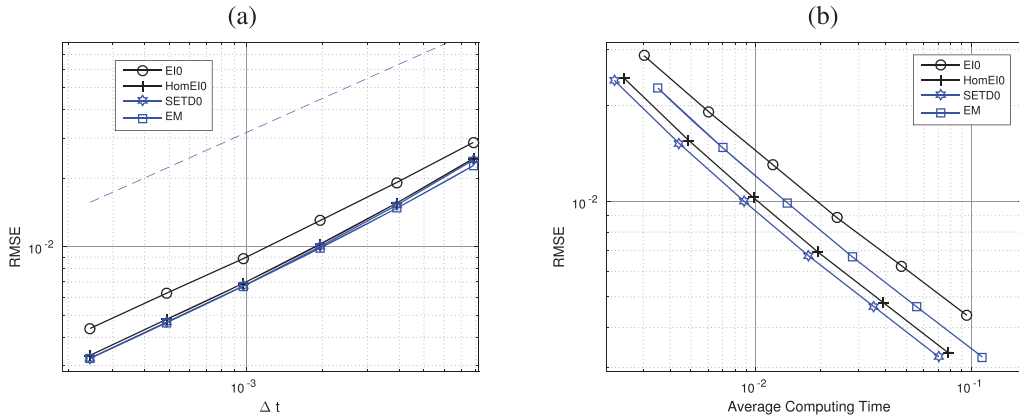


FIG. 9. Euler methods. Equation (4.6) with $\beta = 0.1$, $\alpha = 1$, $r = 4$, $T = 1$ and $M = 1000$ samples (a) RMSE against Δt . Also plotted is a reference line with slope 1/2. (b) RMSE against cputime. The noise is dominated by the nonlinear term. We now see that *SETD0* is the most efficient, followed by *HomEI0*. See Fig. 10 for Milstein type schemes.

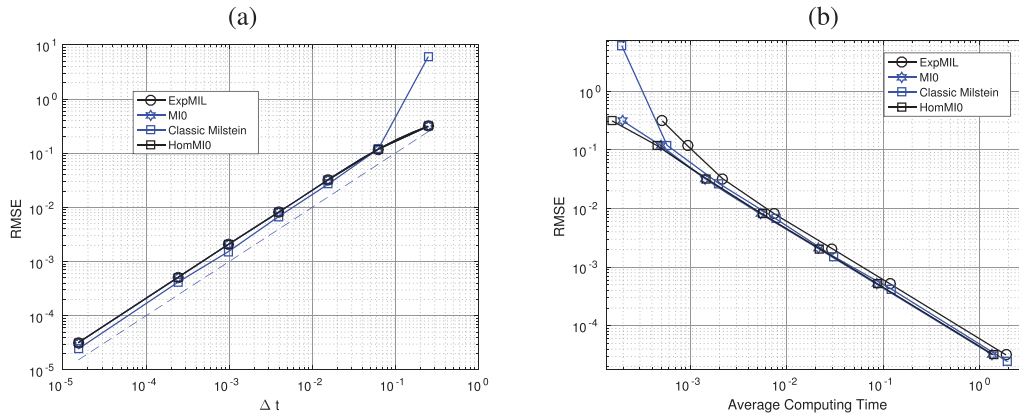


FIG. 10. Milstein methods. Equation (4.6) with $\beta = 0.1$, $\alpha = 1$, $r = 4$, $T = 1$ and $M = 100$ samples (a) RMSE against Δt . Also plotted is a reference line with slope 1 (compare to Fig. 9). In (b) RMSE against cputime. The noise is dominated by the nonlinear term. We see that *HomMIO* and *MIO* are the most efficient.

In order to apply *EI* schemes, consider the splitting

$$G(\mathbf{u}) = \beta \begin{pmatrix} u_1 & 0 & 0 & 0 \\ 0 & u_2 & 0 & 0 \\ 0 & 0 & u_3 & 0 \\ 0 & 0 & 0 & u_4 \end{pmatrix} - \alpha \begin{pmatrix} 0 & 0 & 0 & 0 \\ 0 & u_1 & 0 & 0 \\ 0 & 0 & u_2 & 0 \\ 0 & 0 & 0 & u_3 \end{pmatrix} \quad (4.9)$$

that gives the matrices $B_i = \beta \text{diag}(\mathbf{e}_i)$ and the vectors $\mathbf{g}_i(\mathbf{u})$ having only nonzero element $-\alpha u_i$ in $(i-1)$ th entry. In this case Levy areas are now needed to apply the exponential Milstein scheme. We take a reference step size $\Delta t_{ref} = 2^{-14}$.

Figure 11 compares the cases where $\beta = 1$, $\alpha = 0.1$ in (a) and (b) and $\beta = 1$, $\alpha = 1$ in (c) and (d). When the linear term dominates (Fig. 11(a) and (b)) we see that the schemes *HomEI0* and *EI0* have

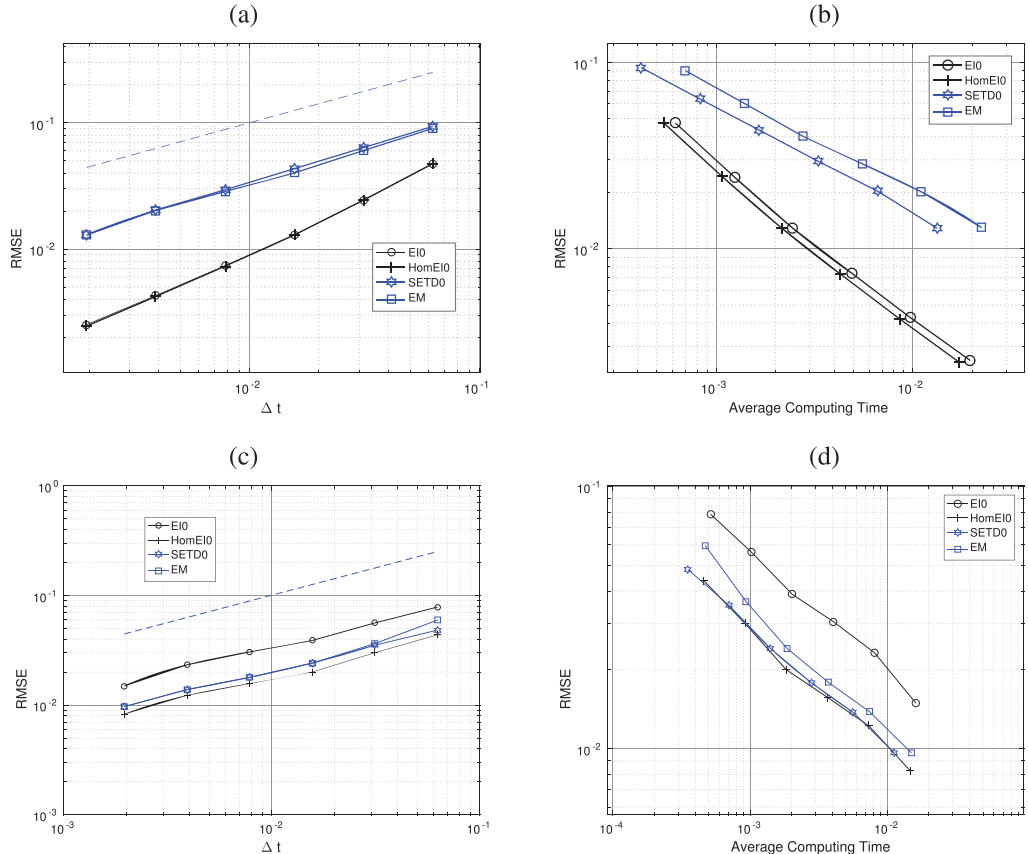


FIG. 11. Equation (4.6) with $r = 4$, $T = 1$ and $M = 100$ samples comparing in (a), (b) $\beta = 1$, $\alpha = 0.1$ and in (c), (d) $\beta = 1$, $\alpha = 1$. (a) and (c) show RMSE against Δt . Also plotted is a reference line with slope $1/2$. (b) and (d) RMSE against cputime. Where the diagonal noise term dominates HomEI0 is the most efficient. For equal weighting we see HomEI0 is as efficient as SETD0.

smaller error and are the most efficient. In Fig. 11(c) and (d), where there is an equal weighting between the diagonal and nondiagonal term in the noise, we see HomEI0 and SETD0 are now equally efficient. When the nondiagonal part dominates the diagonal part of the noise, then Fig. 12 shows that HomEI0 is still the most efficient closely followed by the semiimplicit EM method.

4.4 A finite difference discretization of an SPDE

Let us reconsider the reaction–diffusion equation (4.5) with homogeneous Dirichlet boundary conditions on $(0,1)$. We now take space–time white noise so $W(t)$ is Q -Wiener process on $L^2(0, 1)$ with covariance $Q = I$. Introducing the grid points $x_j = jh$ for $h = 1/J$ and $j = 0, \dots, J$, we denote the standard finite difference approximation of the Laplacian by A . Let $\mathbf{u}_J(t)$ be the solution of the SDE

$$d\mathbf{u}_J = [\varepsilon A\mathbf{u} + \mathbf{f}(\mathbf{u}_J)] dt + [\beta \mathbf{u}_J + \alpha \mathbf{g}(\mathbf{u}_J)] dW_J(t), \quad (4.10)$$

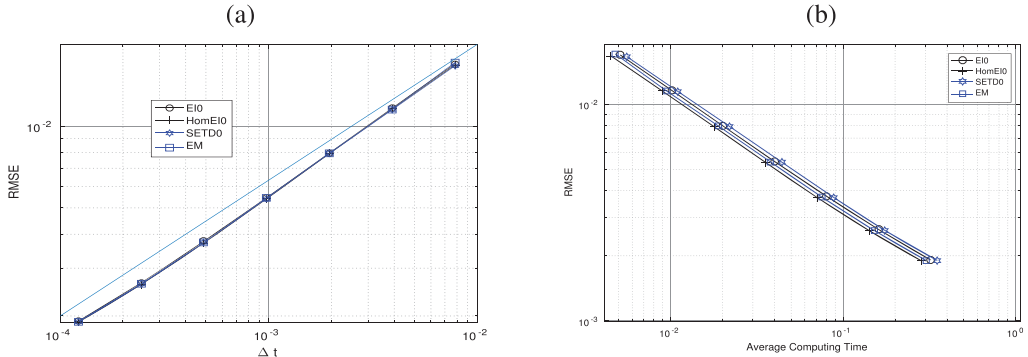


FIG. 12. Equation (4.6) with $r = 4$, $T = 1$ and $M = 1000$ samples with $\beta = 0.1$, $\alpha = 1$. (a) RMSE against Δt . Also plotted is a reference line with slope $1/2$. (b) RMSE against cputime. The noise is dominated by the nondiagonal term and we now see that *HomEI0* is the most efficient, followed by the semiimplicit EM method.

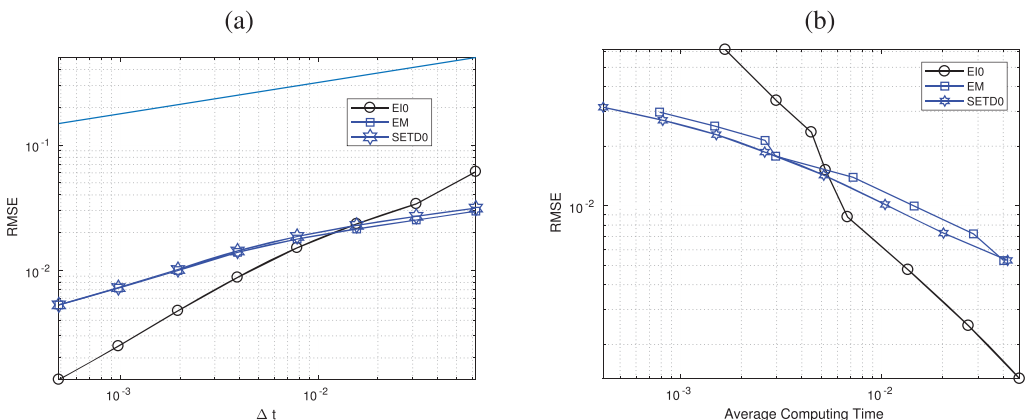


FIG. 13. Euler methods for (4.10) with $\beta = 0.5$, $\alpha = 0$, $T = 1$ and $M = 1000$ samples (a) RMSE against Δt . Also plotted is a reference line with slope $1/2$. In (b) we examine efficiency. We see that *EI0* has an improved rate of convergence and is the most efficient even though commutator conditions (1.2) do not hold. See Fig. 14 for $\alpha > 0$.

where $\mathbf{f}, \mathbf{g} : \mathbb{R}^{J-1} \rightarrow \mathbb{R}^{J-1}$ and $\mathbf{W}_J(t) = [W(t, x_1), W(t, x_2), \dots, W(t, x_{J-1})]^T$. For this finite difference discretization the commutator conditions (1.2) do not hold. So this example (like Section 4.3) is not covered by our theory, unlike the spectral Galerkin discretization in Section 4.2.

First consider the case of linear noise when $\alpha = 0$, in which case *HomEI0* and *EI0* are equivalent. We take $\beta = 0.5$, $T = 1$, $J = 101$ and $M = 1000$. We plot in Fig. 13 the RMSE against Δt in (a) and against cputime in (b). We see that we have an improved rate of convergence for *EI0* and that it is the most efficient of the schemes. When $\alpha = 0.125$, we include the presence of a nonlinear term in the noise, and results are shown in Fig. 14. We still have an improved rate of convergence, and now *HomEI0* is more slightly more accurate and efficient than *EI0*.

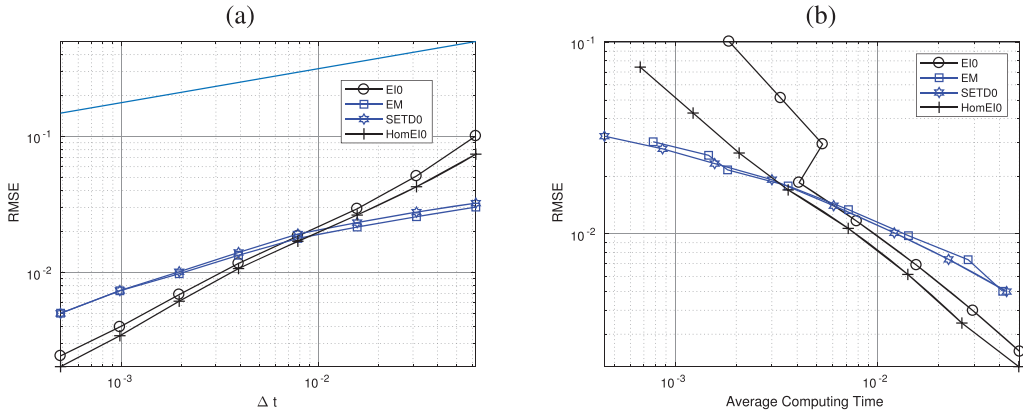


FIG. 14. Euler methods for (4.10) with $\beta = 0.5$, $\alpha = 0.125$, $T = 1$ and $M = 1000$ samples (a) RMSE against Δt . Also plotted is a reference line with slope 1/2. (b) RMSE against cputime. We see that $EI0$ and $HomEI0$ have an improved rate of convergence and are the most efficient. See Fig. 13 for $\alpha = 0$.

5. Proofs of the main results

Before giving the proofs of Theorems 3.1 and 3.2, we recall the following Proposition, see for example, Lord *et al.* (2014) for the proof.

PROPOSITION 5.1 Let Assumption 1 hold. For each $T > 0$ and $\mathbf{u}(0) = \mathbf{u}_0 \in \mathbb{R}^d$ there exists a unique \mathbf{u} satisfying (1.1) such that

$$\sup_{t \in [0, T]} \|\mathbf{u}(t)\|_{L^2(\Omega, \mathbb{R}^d)} = \sup_{t \in [0, T]} \mathbb{E} \left[\|\mathbf{u}(t)\|_2^2 \right]^{1/2} < \infty.$$

Furthermore, there exists $K > 0$ such that for $0 \leq s, t \leq T$

$$\|\mathbf{u}(t) - \mathbf{u}(s)\|_{L^2(\Omega, \mathbb{R}^d)} \leq K|t - s|^{1/2}. \quad (5.1)$$

LEMMA 5.1 The semigroup operator $\Phi_{t,s}$ given in (2) and $\Phi_{t,s}^{-1}$ satisfy the following: given $\mathbf{v} \in L^2(\Omega, \mathbb{R}^d)$

$$\|\Phi_{t,s}\mathbf{v}\|_{L^2(\Omega, \mathbb{R}^d)}^2 \leq \mathbb{E} \left[\|\Phi_{t,s}\|_2^2 \right] \|\mathbf{v}\|_{L^2(\Omega, \mathbb{R}^d)}^2 \quad \text{and} \quad \|\Phi_{t,s}^{-1}\mathbf{v}\|_{L^2(\Omega, \mathbb{R}^d)}^2 \leq \mathbb{E} \left[\|\Phi_{t,s}^{-1}\|_2^2 \right] \|\mathbf{v}\|_{L^2(\Omega, \mathbb{R}^d)}^2,$$

where $\|\Phi_{t,s}\|_2 = \sup_{\|\mathbf{x}\|_2=1} \|\Phi_{t,s}\mathbf{x}\|_2$ for $\mathbf{x} \in \mathbb{R}^d$. Furthermore,

$$\sup_{t,s \in [0, T]} \mathbb{E} \left[\|\Phi_{t,s}\|_2^2 \right] < \infty \quad \text{and} \quad \sup_{t,s \in [0, T]} \mathbb{E} \left[\|\Phi_{t,s}^{-1}\|_2^2 \right] < \infty.$$

Proof. Note that $\|\Phi_{t,s}\mathbf{v}\|_2^2 \leq \|\Phi_{t,s}\|_2^2 \|\mathbf{v}\|_2^2$ and, taking the expectation and applying the Cauchy-Schwarz inequality with the inequality $E[X^4] \leq E[X^2]^2$ (Pons, 2016), give the first inequality.

A straightforward calculation reveals

$$\begin{aligned}\mathbb{E} \left[\|\Phi_{t,s}\|_2^2 \right] &\leqslant e^{2\mathbb{E} \left[\left\| \left(A - \frac{1}{2} \sum_{i=1}^m B_i^2 \right) (t-s) + \sum_{i=1}^m B_i (W_i(t) - W_i(s)) \right\|_2 \right]} \\ &\leqslant e^{2 \left\| A - \frac{1}{2} \sum_{i=1}^m B_i^2 \right\|_2 |t-s| + 2 \sum_{i=1}^m \|B_i\|_2 \sqrt{\frac{2|t-s|}{\pi}}},\end{aligned}$$

which means that $\Phi_{t,s}$ and $\Phi_{t,s}^{-1}$ are uniformly bounded for $t, s \in [0, T]$. \square

From now on we let

$$C = \max \left\{ \sup_{s,t \in [0,T]} \mathbb{E} \left[\|\Phi_{s,t}\|_2^2 \right], \sup_{s,t \in [0,T]} \mathbb{E} \left[\|\Phi_{s,t}^{-1}\|_2^2 \right] \right\}.$$

We now start to examine the remainder terms that arise from the local error. Let us define the map for the exact flow

$$\Psi_{\text{Exact}}(t_{k+1}, t_k, \mathbf{u}(t_k)) = \Phi_{t_{k+1}, t_k} \left[\mathbf{u}(t_k) + \int_{t_k}^{t_{k+1}} \Phi_{s, t_k}^{-1} \tilde{\mathbf{f}}(\mathbf{u}(s)) ds + \sum_{i=1}^m \int_{t_k}^{t_{k+1}} \Phi_{s, t_k}^{-1} \mathbf{g}_i(\mathbf{u}(s)) dW_i(s) \right]. \quad (5.2)$$

This exact flow will be used in the analysis of *EI0*. However to analyse *MIO*, it is more convenient to use the following Ito–Taylor expansion (see (2.8)):

$$\begin{aligned}\Psi_{\text{Exact}}(t_{k+1}, t_k, \mathbf{u}(t_k)) &= \Phi_{t_{k+1}, t_k} \left[\mathbf{u}(t_k) + \int_{t_k}^{t_{k+1}} \Phi_{s, t_k}^{-1} \tilde{\mathbf{f}}(\mathbf{u}(s)) ds + \sum_{i=1}^m \int_{t_k}^{t_{k+1}} \mathbf{g}_i(\mathbf{u}(t_k)) dW_i(s) \right] \\ &+ \sum_{i=1}^m \sum_{l=1}^m \int_{t_k}^{t_{k+1}} \int_{t_k}^s \Phi_{r, t_k}^{-1} \mathbf{H}_{i,l}(\mathbf{u}(r)) dW_l(r) dW_i(s) + \sum_{i=1}^m \int_{t_k}^{t_{k+1}} \int_{t_k}^s \Phi_{r, t_k}^{-1} \mathbf{Q}_i(\mathbf{u}(r)) dr dW_i(s).\end{aligned} \quad (5.3)$$

The numerical flows for *EI0* and *MIO* are given by

$$\Psi_{\text{EI0}}(t_{k+1}, t_k, \mathbf{u}(t_k)) = \Phi_{t_{k+1}, t_k} \mathbf{u}(t_k) + \Phi_{t_{k+1}, t_k} \int_{t_k}^{t_{k+1}} \tilde{\mathbf{f}}(\mathbf{u}(t_k)) ds + \sum_{i=1}^m \Phi_{t_{k+1}, t_k} \int_{t_k}^{t_{k+1}} \mathbf{g}_i(\mathbf{u}(t_k)) dW_i(s) \quad (5.4)$$

and

$$\Psi_{\text{MIO}}(t_{k+1}, t_k, \mathbf{u}(t_k)) = \Psi_{\text{EI0}}(t_{k+1}, t_k, \mathbf{u}(t_k)) + \sum_{i=1}^m \sum_{l=1}^m \Phi_{t_{k+1}, t_k} \int_{t_k}^{t_{k+1}} \int_{t_k}^s \mathbf{H}_{i,l}(\mathbf{u}(t_k)) dW_l(r) dW_i(s). \quad (5.5)$$

5.1 Proof of Theorem 3.1

First we look at the local error $R_{EI0} = \Psi_{\text{Exact}}(t, s, \mathbf{u}(s)) - \Psi_{EI0}(t, s, \mathbf{u}(s))$ for $EI0$.

LEMMA 5.2 Let Assumption 1 hold. Then

$$\left\| \sum_{k=0}^{N-1} \Phi_{t_N, t_{k+1}} R_{EI0}(t_{k+1}, t_k, \mathbf{u}(t_k)) \right\|_{L^2(\Omega, \mathbb{R}^d)}^2 = \mathcal{O}(\Delta t).$$

Proof. Considering the exact flow (5.2) and the numerical flow (5.4), the local error of $EI0$ is given by

$$\begin{aligned} R_{EI0}(t_{k+1}, t_k, \mathbf{u}(t_k)) &= \Phi_{t_{k+1}, t_k} \int_{t_k}^{t_{k+1}} \left(\Phi_{s, t_k}^{-1} \tilde{\mathbf{f}}(\mathbf{u}(s)) - \tilde{\mathbf{f}}(\mathbf{u}(t_k)) \right) ds \\ &\quad + \sum_{i=1}^m \Phi_{t_{k+1}, t_k} \int_{t_k}^{t_{k+1}} \left(\Phi_{s, t_k}^{-1} \mathbf{g}_i(\mathbf{u}(s)) - \mathbf{g}_i(\mathbf{u}(t_k)) \right) dW_i(s). \end{aligned} \quad (5.6)$$

Adding and subtracting the terms $\Phi_{s, t_k}^{-1} \tilde{\mathbf{f}}(\mathbf{u}(t_k))$, and $\Phi_{s, t_k}^{-1} \mathbf{g}_i(\mathbf{u}(t_k))$ in the first and second integrals, we have

$$\begin{aligned} &\left\| \sum_{k=0}^{N-1} \Phi_{t_N, t_{k+1}} R_{EI0}(t_{k+1}, t_k, \mathbf{u}(t_k)) \right\|_{L^2(\Omega, \mathbb{R}^d)}^2 \\ &\leq 4 \left\| \sum_{k=0}^{N-1} \Phi_{t_N, t_k} \int_{t_k}^{t_{k+1}} \Phi_{s, t_k}^{-1} (\tilde{\mathbf{f}}(\mathbf{u}(s)) - \tilde{\mathbf{f}}(\mathbf{u}(t_k))) ds \right\|_{L^2(\Omega, \mathbb{R}^d)}^2 \\ &\quad + 4 \left\| \sum_{k=0}^{N-1} \Phi_{t_N, t_k} \int_{t_k}^{t_{k+1}} \left(\Phi_{s, t_k}^{-1} \tilde{\mathbf{f}}(\mathbf{u}(t_k)) - \tilde{\mathbf{f}}(\mathbf{u}(t_k)) \right) ds \right\|_{L^2(\Omega, \mathbb{R}^d)}^2 \\ &\quad + 4 \left\| \sum_{k=0}^{N-1} \Phi_{t_N, t_k} \sum_{i=1}^m \int_{t_k}^{t_{k+1}} \Phi_{s, t_k}^{-1} (\mathbf{g}_i(\mathbf{u}(s)) - \mathbf{g}_i(\mathbf{u}(t_k))) dW_i(s) \right\|_{L^2(\Omega, \mathbb{R}^d)}^2 \\ &\quad + 4 \left\| \sum_{k=0}^{N-1} \Phi_{t_N, t_k} \sum_{i=1}^m \int_{t_k}^{t_{k+1}} \left(\Phi_{s, t_k}^{-1} \mathbf{g}_i(\mathbf{u}(t_k)) - \mathbf{g}_i(\mathbf{u}(t_k)) \right) dW_i(s) \right\|_{L^2(\Omega, \mathbb{R}^d)}^2 \\ &= I + II + III + IV. \end{aligned}$$

We now consider each of the terms I , II , III , IV separately. We start with I by applying Jensen's inequality for sums and Lemma 5.1

$$\begin{aligned} I &\leq 4N \sum_{k=0}^{N-1} \left\| \Phi_{t_N, t_k} \int_{t_k}^{t_{k+1}} \Phi_{s, t_k}^{-1} (\tilde{\mathbf{f}}(\mathbf{u}(s)) - \tilde{\mathbf{f}}(\mathbf{u}(t_k))) ds \right\|_{L^2(\Omega, \mathbb{R}^d)}^2 \\ &\leq 4NC \sum_{k=0}^{N-1} \mathbb{E} \left[\left\| \int_{t_k}^{t_{k+1}} \Phi_{s, t_k}^{-1} (\tilde{\mathbf{f}}(\mathbf{u}(s)) - \tilde{\mathbf{f}}(\mathbf{u}(t_k))) ds \right\|_2^2 \right]. \end{aligned}$$

Now using Jensen's inequality for the integral, the global Lipschitz property of $\tilde{\mathbf{f}}$, Lemma 5.1 and Proposition 5.1, we get

$$\begin{aligned} I &\leqslant 4N\Delta t C \sum_{k=0}^{N-1} \int_{t_k}^{t_{k+1}} \mathbb{E} \left[\left\| \boldsymbol{\Phi}_{s,t_k}^{-1} (\tilde{\mathbf{f}}(\mathbf{u}(s)) - \tilde{\mathbf{f}}(\mathbf{u}(t_k))) \right\|_2^2 \right] ds \\ &\leqslant 4TC^2 L^2 \sum_{k=0}^{N-1} \int_{t_k}^{t_{k+1}} \mathbb{E} \left[\|(\mathbf{u}(s) - \mathbf{u}(t_k))\|_2^2 \right] ds \\ &\leqslant 4TC^2 L^2 K^2 \sum_{k=0}^{N-1} \int_{t_k}^{t_{k+1}} |s - t_k| ds = K_I \Delta t. \end{aligned}$$

For II , it is straightforward to see $II \leqslant K_{II} \Delta t$ by considering the fact that $\mathbb{E} \left[\left\| (\boldsymbol{\Phi}_{s,t_k}^{-1} - I) \mathbf{v} \right\|_2^2 \right] \leqslant K|s - t_k|$ for any \mathcal{F}_{t_k} measurable $\mathbf{v} \in L^2(\Omega, \mathbb{R}^d)$. This follows since $\mathbf{u}(t) = \boldsymbol{\Phi}_{s,t_k}^{-1} \mathbf{v}$ is the solution of the SDE

$$d\mathbf{u} = \left(-A + \sum_{i=1}^m B_i \right) \mathbf{u}(t) dt - \sum_{i=1}^m B_i \mathbf{u}(t) dW_i(t), \quad \mathbf{u}(t_k) = \mathbf{v}$$

satisfying assumptions of Proposition 5.1.

For the term III ,

$$III = 4 \left\| \boldsymbol{\Phi}_{t_N,0} \sum_{k=0}^{N-1} \sum_{i=1}^m \int_{t_k}^{t_{k+1}} \boldsymbol{\Phi}_{s,0}^{-1} (\mathbf{g}_i(\mathbf{u}(s)) - \mathbf{g}_i(\mathbf{u}(t_k))) dW_i(s) \right\|_{L^2(\Omega, \mathbb{R}^d)}^2,$$

where $\boldsymbol{\Phi}_{t_N,t_k} = \boldsymbol{\Phi}_{t_N,0} \boldsymbol{\Phi}_{t_k,0}^{-1}$ is due to commutativity of the matrices A and B_i , $i = 1, \dots, m$. We have by the Ito isometry

$$\begin{aligned} III &\leqslant 4C \sum_{k=0}^{N-1} \sum_{i=1}^m \int_{t_k}^{t_{k+1}} \mathbb{E} \left[\left\| \boldsymbol{\Phi}_{s,0}^{-1} (\mathbf{g}_i(\mathbf{u}(s)) - \mathbf{g}_i(\mathbf{u}(t_k))) \right\|_2^2 \right] ds \\ &\leqslant 4C^2 L^2 K^2 m \sum_{k=0}^{N-1} \int_{t_k}^{t_{k+1}} |s - t_k| ds = \mathcal{O}(\Delta t), \end{aligned}$$

where the global Lipschitz property of \mathbf{g}_i , Proposition 5.1 and Lemma 5.1 is used. By a similar argument we have $IV = \mathcal{O}(\Delta t)$. Combining I , II , III and IV we obtain the result. \square

Proof of Theorem 3.1. By induction, we can express the approximation of $\mathbf{u}(t_N)$ by \mathbf{u}_N found by EI0 at $t = t_N$ as

$$\mathbf{u}_N = \boldsymbol{\Phi}_{t_N,0} \mathbf{u}_0 + \sum_{k=0}^{N-1} \boldsymbol{\Phi}_{t_N,t_k} \int_{t_k}^{t_{k+1}} \tilde{\mathbf{f}}(\mathbf{u}_k) ds + \sum_{k=0}^{N-1} \sum_{i=1}^m \boldsymbol{\Phi}_{t_N,t_k} \int_{t_k}^{t_{k+1}} \mathbf{g}_i(\mathbf{u}_k) dW_i(s). \quad (5.7)$$

Due to commutativity of the matrices A and B_i 's, $\Phi_{t_N, t_k} = \Phi_{t_N, 0} \Phi_{t_k, 0}^{-1}$, the matrix $\Phi_{t_k, 0}^{-1}$ can be taken inside the integrals. Now we define the continuous time process $\mathbf{u}_{\Delta t}(t)$ for (5.7) that agrees with approximation \mathbf{u}_k at $t = t_k$. By introducing the variable $\hat{t} = t_k$ for $t_k \leq t < t_{k+1}$,

$$\mathbf{u}_{\Delta t}(t) = \Phi_{t, 0} \mathbf{u}_{\Delta t}(0) + \Phi_{t, 0} \int_0^t \Phi_{\hat{s}, 0}^{-1} \tilde{\mathbf{f}}(\mathbf{u}_{\Delta t}(\hat{s})) \, ds + \sum_{i=1}^m \Phi_{t, 0} \int_0^t \Phi_{\hat{s}, 0}^{-1} \mathbf{g}_i(\mathbf{u}_{\Delta t}(\hat{s})) \, dW_i(s).$$

This continuous version has the property that $\mathbf{u}_{\Delta t}(t_k) = \mathbf{u}_k$. By recalling the definition of the local error, the iterated sum of the exact solution at $t = t_N$ is found by induction to be

$$\begin{aligned} \mathbf{u}(t_N) &= \Phi_{t_N, 0} \mathbf{u}_0 + \Phi_{t_N, 0} \int_0^{t_N} \Phi_{\hat{s}, 0}^{-1} \tilde{\mathbf{f}}(\mathbf{u}(\hat{s})) \, ds \\ &\quad + \Phi_{t_N, 0} \sum_{i=1}^m \int_0^{t_N} \Phi_{\hat{s}, 0}^{-1} \mathbf{g}_i(\mathbf{u}(\hat{s})) \, dW_i(s) + \sum_{k=0}^{N-1} \Phi_{t_N, t_{k+1}} R_{EI0}(t_{k+1}, t_k, \mathbf{u}(t_k)). \end{aligned} \quad (5.8)$$

Denoting the error by $\mathbf{e}(\hat{t}) = \mathbf{u}(\hat{t}) - \mathbf{u}_{\Delta t}(\hat{t})$, we see that

$$\|\mathbf{e}(\hat{t})\|_{L^2(\Omega, \mathbb{R}^d)}^2 \leq \left(3\hat{t}C^2L^2 + 3C^2mL^2 \right) \int_0^{\hat{t}} \mathbb{E} \left[\|\mathbf{e}(s)\|_2^2 \right] \, ds + 3K_{EI0}\Delta t,$$

where L is the largest one of the Lipschitz constants of the functions \mathbf{g}_i , $\tilde{\mathbf{f}}$. Finally, Gronwall's inequality completes the proof.

5.2 Proof of Theorem 3.2

We now examine the local error for *MIO*, given by (2.11).

LEMMA 5.3 Let Assumptions 1 and 2 and 3 hold. Then

$$\left\| \sum_{k=0}^{N-1} \Phi_{t_N, t_{k+1}} R_{MIO}(t_{k+1}, t_k, \mathbf{u}(t_k)) \right\|_{L^2(\Omega, \mathbb{R}^d)}^2 = \mathcal{O}(\Delta t^2), \quad (5.9)$$

where $R_{MIO}(t, s, \mathbf{u}(s)) = \Psi_{\text{Exact}}(t, s, \mathbf{u}(s)) - \Psi_{MIO}(t, s, \mathbf{u}(s))$.

Proof. Considering the exact flow (5.3) and the numerical flow (5.5) corresponding to the scheme *MIO*, we have

$$\begin{aligned} R_{MIO}(t_{k+1}, t_k, \mathbf{u}(t_k)) &= \Phi_{t_{k+1}, t_k} \int_{t_k}^{t_{k+1}} \left(\Phi_{s, t_k}^{-1} \tilde{\mathbf{f}}(\mathbf{u}(s)) - \tilde{\mathbf{f}}(\mathbf{u}(t_k)) \right) \, ds \\ &\quad + \sum_{i=1}^m \sum_{l=1}^m \Phi_{t_{k+1}, t_k} \int_{t_k}^{t_{k+1}} \int_{t_k}^s \left(\Phi_{r, t_k}^{-1} \mathbf{H}_{i,l}(\mathbf{u}(r)) - \mathbf{H}_{i,l}(\mathbf{u}(t_k)) \right) \, dW_l(r) \, dW_i(s) \\ &\quad + \sum_{i=1}^m \Phi_{t_{k+1}, t_k} \int_{t_k}^{t_{k+1}} \int_{t_k}^s \Phi_{r, t_k}^{-1} \mathbf{Q}_i(\mathbf{u}(r)) \, dr \, dW_i(s). \end{aligned} \quad (5.10)$$

Adding and subtracting the terms $\Phi_{s,t_k}^{-1}\tilde{\mathbf{f}}(\mathbf{u}(t_k))$, $\Phi_{s,t_k}^{-1}\mathbf{H}_{i,l}(\mathbf{u}(t_k))$ in the first and second integrals respectively, and summing and taking the norm and applying Jensen's inequality, we have

$$\left\| \sum_{k=0}^{N-1} \Phi_{t_N, t_{k+1}} R_{MIO}(t_{k+1}, t_k, \mathbf{u}(t_k)) \right\|_{L^2(\Omega, \mathbb{R}^d)}^2 \leq I + II + III + IV + V$$

with

$$\begin{aligned} I &:= 5 \left\| \sum_{k=0}^{N-1} \Phi_{t_N, t_k} \int_{t_k}^{t_{k+1}} \Phi_{s, t_k}^{-1} (\tilde{\mathbf{f}}(\mathbf{u}(s)) - \tilde{\mathbf{f}}(\mathbf{u}(t_k))) \, ds \right\|_{L^2(\Omega, \mathbb{R}^d)}^2 \\ II &:= 5 \left\| \sum_{k=0}^{N-1} \Phi_{t_N, t_k} \int_{t_k}^{t_{k+1}} (\Phi_{s, t_k}^{-1} \tilde{\mathbf{f}}(\mathbf{u}(t_k)) - \tilde{\mathbf{f}}(\mathbf{u}(t_k))) \, ds \right\|_{L^2(\Omega, \mathbb{R}^d)}^2 \\ III &:= 5 \left\| \sum_{k=0}^{N-1} \sum_{i=1}^m \sum_{l=1}^m \Phi_{t_N, t_k} \int_{t_k}^{t_{k+1}} \int_{t_k}^s \Phi_{r, t_k}^{-1} (\mathbf{H}_{i,l}(\mathbf{u}(r)) - \mathbf{H}_{i,l}(\mathbf{u}(t_k))) \, dW_l(r) \, dW_i(s) \right\|_{L^2(\Omega, \mathbb{R}^d)}^2 \\ IV &:= 5 \left\| \sum_{k=0}^{N-1} \sum_{i=1}^m \sum_{l=1}^m \Phi_{t_N, t_k} \int_{t_k}^{t_{k+1}} \int_{t_k}^s (\Phi_{r, t_k}^{-1} \mathbf{H}_{i,l}(\mathbf{u}(t_k)) - \mathbf{H}_{i,l}(\mathbf{u}(t_k))) \, dW_l(r) \, dW_i(s) \right\|_{L^2(\Omega, \mathbb{R}^d)}^2 \end{aligned}$$

and remainder

$$V =: 5 \left\| \sum_{k=0}^{N-1} \sum_{i=1}^m \Phi_{t_N, t_k} \int_{t_k}^{t_{k+1}} \int_{t_k}^s \Phi_{r, t_k}^{-1} \mathbf{Q}_i(\mathbf{u}(r)) \, dr \, dW_i(s) \right\|_{L^2(\Omega, \mathbb{R}^d)}^2.$$

We now consider each of the terms I, II, III, IV, V separately and we start with I . By Assumption 3, we have the following Ito–Taylor expansion for $\tilde{\mathbf{f}}$

$$\begin{aligned} \tilde{\mathbf{f}}(\mathbf{u}(s)) &= \tilde{\mathbf{f}}(\mathbf{u}(t_k)) + \sum_{i=1}^m D\tilde{\mathbf{f}}(\mathbf{u}(t_k)) (B_i \mathbf{u}(t_k) + \mathbf{g}_i(\mathbf{u}(t_k))) (W_i(s) - W_i(t_k)) + R_{\tilde{f}} \\ &= \tilde{\mathbf{f}}(\mathbf{u}(t_k)) + \sum_{i=1}^m \mathbf{K}_i (W_i(s) - W_i(t_k)) + R_{\tilde{f}}. \end{aligned}$$

We know that $R_{\tilde{f}} = \mathcal{O}(s - t_k)$, see for example Lord *et al.* (2014). By Jensen's inequality for the sum and Ito–Taylor expansion,

$$\begin{aligned} I &\leq 10 \mathbb{E} \left[\left\| \sum_{k=0}^{N-1} \int_{t_k}^{t_{k+1}} \Phi_{t_N, s} \left(\sum_{i=1}^m \mathbf{K}_i (W_i(s) - W_i(t_k)) \right) \, ds \right\|_2^2 \right] \\ &\quad + 10 \mathbb{E} \left[\left\| \sum_{k=0}^{N-1} \int_{t_k}^{t_{k+1}} \Phi_{t_N, s} R_{\tilde{f}} \, ds \right\|_2^2 \right]. \end{aligned}$$

By Lemma 5.1 for $\Phi_{t_N, s}$, we have

$$I \leq 10C\mathbb{E} \left[\left\| \sum_{k=0}^{N-1} \int_{t_k}^{t_{k+1}} \left(\sum_{i=1}^m \mathbf{K}_i (W_i(s) - W_i(t_k)) \right) ds \right\|_2^2 \right] + 10C\mathbb{E} \left[\left\| \sum_{k=0}^{N-1} \int_{t_k}^{t_{k+1}} R_{\tilde{f}} ds \right\|_2^2 \right].$$

Let us write $I \leq I_a + I_b$, representing the first and second term by I_a and I_b , respectively, and investigate the first term I_a . By the orthogonality relation $\mathbb{E} [\langle \Theta_k, \Theta_l \rangle] = 0$, $k \neq l$ for

$$\Theta_k = \int_{t_k}^{t_{k+1}} \left(\sum_{i=1}^m \mathbf{K}_i (W_i(s) - W_i(t_k)) \right) ds,$$

we have

$$I_a = 10C \sum_{k=0}^{N-1} \mathbb{E} \left[\left\| \int_{t_k}^{t_{k+1}} \left(\sum_{i=1}^m \mathbf{K}_i (W_i(s) - W_i(t_k)) \right) ds \right\|_2^2 \right].$$

By two applications of Jensen's inequality for the integral and sum

$$I_a \leq 10CmK\Delta t \sup_{i \in \{1, \dots, m\}} \mathbb{E} [\|\mathbf{K}_i\|_2]^2 \sum_{k=0}^{N-1} \sum_{i=1}^m \int_{t_k}^{t_{k+1}} \mathbb{E} [\|W_i(s) - W_i(t_k)\|_2^2] ds = \mathcal{O}(\Delta t^2).$$

Since R_f contains higher order terms, we conclude $I = \mathcal{O}(\Delta t^2)$. Similarly, for II we find the same order by following same arguments.

For III , we have by the Ito isometry applied consecutively for outer and inner stochastic integrals

$$\begin{aligned} III &\leq 5C \left\| \sum_{k=0}^{N-1} \sum_{i=1}^m \sum_{l=1}^m \int_{t_k}^{t_{k+1}} \int_{t_k}^s \Phi_{r,0}^{-1} (\mathbf{H}_{i,l}(\mathbf{u}(r)) - \mathbf{H}_{i,l}(\mathbf{u}(t_k))) dW_l(r) dW_i(s) \right\|_{L^2(\Omega, \mathbb{R}^d)}^2 \\ &= 5C \sum_{k=0}^{N-1} \sum_{i=1}^m \int_{t_k}^{t_{k+1}} \mathbb{E} \left[\left\| \left(\sum_{l=1}^m \int_{t_k}^s \Phi_{r,0}^{-1} (\mathbf{H}_{i,l}(\mathbf{u}(r)) - \mathbf{H}_{i,l}(\mathbf{u}(t_k))) dW_l(r) \right) \right\|_2^2 \right] ds \\ &= 5C \sum_{k=0}^{N-1} \sum_{i=1}^m \sum_{l=1}^m \int_{t_k}^{t_{k+1}} \int_{t_k}^s \mathbb{E} \left[\left\| \Phi_{r,0}^{-1} (\mathbf{H}_{i,l}(\mathbf{u}(r)) - \mathbf{H}_{i,l}(\mathbf{u}(t_k))) \right\|_2^2 \right] dr ds. \end{aligned}$$

By the global Lipschitz property of $\mathbf{H}_{i,l}$, Proposition 5.1 and Lemma 5.1

$$III \leq K_{III} \sum_{k=0}^{N-1} \int_{t_k}^{t_{k+1}} \int_{t_k}^s |r - t_k| dr ds = K_{III} \Delta t^2.$$

In a similar way, it can be shown that $IV \leq K_{IV} \Delta t^2$. Since $\int_{t_k}^{t_{k+1}} \int_{t_k}^s dr dW(s) \sim N(0, \frac{1}{3} \Delta t^3)$, it is straightforward to see $V \leq K_V \Delta t^2$. \square

Proof of Theorem 3.2 As in the proof of Theorem 3.1, we define the continuous time process $\mathbf{u}_{\Delta t}(t)$ for MIO that agrees with approximation \mathbf{u}_k at $t = t_k$. By introducing the variable $\hat{t} = t_k$ for $t_k \leq t < t_{k+1}$,

$$\begin{aligned}\mathbf{u}_{\Delta t}(t) = & \Phi_{t,0}\mathbf{u}_{\Delta t}(0) + \Phi_{t,0}\int_0^t \Phi_{\hat{s},0}^{-1}\tilde{\mathbf{f}}(\mathbf{u}_{\Delta t}(\hat{s})) \, ds + \sum_{i=1}^m \Phi_{t,0}\int_0^t \Phi_{\hat{s},0}^{-1}\mathbf{g}_i(\mathbf{u}_{\Delta t}(\hat{s})) \, dW_i(s) \\ & + \sum_{i=1}^m \sum_{l=1}^m \Phi_{t,0}\int_0^t \int_{\hat{s}}^s \Phi_{\hat{s},0}^{-1}\mathbf{H}_{i,l}(\mathbf{u}_{\Delta t}(\hat{s})) \, dW_l(r) \, dW_i(s).\end{aligned}\quad (5.11)$$

The iterated sum of the exact solution at $t = t_N$ is obtained inductively to be

$$\begin{aligned}\mathbf{u}(t_N) = & \Phi_{t_N,0}\mathbf{u}_0 + \Phi_{t_N,0}\int_0^{t_N} \Phi_{\hat{s},0}^{-1}\tilde{\mathbf{f}}(\mathbf{u}(\hat{s})) \, ds + \Phi_{t_N,0}\sum_{i=1}^m \int_0^{t_N} \Phi_{\hat{s},0}^{-1}\mathbf{g}_i(\mathbf{u}(\hat{s})) \, dW_i(s) \\ & + \sum_{i=1}^m \sum_{l=1}^m \Phi_{t_N,0}\int_0^{t_N} \int_{\hat{s}}^s \Phi_{\hat{s},0}^{-1}\mathbf{H}_{i,l}(\mathbf{u}(\hat{s})) \, dW_l(r) \, dW_i(s) + \sum_{k=0}^{N-1} \Phi_{t_N,t_{k+1}}R_{MIO}(t_{k+1}, t_k, \mathbf{u}(t_k)).\end{aligned}\quad (5.12)$$

Denoting the error by $\mathbf{e}(\hat{t}) = \mathbf{u}(\hat{t}) - \mathbf{u}_{\Delta t}(\hat{t})$, we see that

$$\|\mathbf{e}(\hat{t})\|_{L^2(\Omega, \mathbb{R}^d)}^2 \leq \left(4\hat{t}C^2L^2 + 4C^2L^2m(1+m)\right) \int_0^{\hat{t}} \mathbb{E}\left[\|\mathbf{e}(s)\|_2^2\right] \, ds + 4K_{MIO}\Delta t^2.$$

Finally, Gronwall's inequality completes the proof.

6. Conclusion and remarks

Exponential integrators that take advantage of the exact solution of Geometric Brownian Motion have been derived and strong convergence proved. Weak convergence of these numerical methods is under investigation and numerically we observe convergence of $\mathcal{O}(\Delta t)$ (as would be expected). The proposed schemes are particularly well suited to SDEs arising from the spectral Galerkin discretization of an SPDE, see Section 4.2, where typically diagonal noise arises and the zero commutator conditions (1.2) hold. The homotopy based scheme we introduced can take advantage of linearity in the diffusion and at the same time effectively handle nonlinear noise. Where the SDEs are not of the semilinear form of (1.1) then a Rosenbrock type method could be applied, similar to Hochbruck *et al.* (2009). The numerical results of Section 4.3 and Section 4.4 examine cases where the zero commutator conditions fail. Our numerical examples show that these new exponential-based schemes remain more efficient than the standard integrators.

We have seen in this work the effectiveness of the homotopy approach with the simple choice of parameter in (4.2), and it would be interesting to investigate an adaptive choice in the future; preliminary work suggests that this can further increase the efficiency.

Acknowledgements

We would like to thank Raphael Kruse for his comments on an earlier draft.

Funding

The first author was supported by Tubitak grant: 2219 International Post-Doctoral Research Fellowship Programme. Work was completed at the Department of Mathematics, Maxwell Institute, Heriot Watt University, UK, whilst on leave from the Department of Mathematics, Uşak University, Turkey.

REFERENCES

- BECKER, S., JENTZEN, A. & KLOEDEN, P. (2016) An exponential Wagner–Platen type scheme for SPDEs. *SIAM J. Numer. Anal.*, **54**, 2389–2426.
- BISCAY, R., JIMENEZ, J., RIERA, J. & VALDES, P. (1996) Local linearization method for the numerical solution of stochastic differential equations. *Ann. Inst. Stat. Math.*, **48**, 631–644.
- BUCKWAR, E. & KELLY, C. (2010) Towards a systematic linear stability analysis of numerical methods for systems of stochastic differential equations. *SIAM J. Numer. Anal.*, **48**, 298–321.
- CARBONELL, F. & JIMENEZ, J. C. (2008) Weak local linear discretizations for stochastic differential equations with jumps. *J. Appl. Probab.*, **45**, 201–210.
- HASEGAWA, H. (2008) Stochastic bifurcation in FitzHugh-Nagumo ensembles subjected to additive and/or multiplicative noises. *Phys. D: Nonlin. Phenomena*, **237**, 137–155.
- HOCHBRUCK, M., OSTERMANN, A. & SCHWEITZER, J. (2009) Exponential Rosenbrock-type methods. *SIAM J. Numer. Anal.*, **47**, 786–803.
- HOCHBRUCK, M. & OSTERMANN, A. (2010) Exponential integrators. *Acta Numerica*, **19**, 209–286.
- HUTZENTHALER, M. & JENTZEN, A. (2015) *Numerical Approximations of Stochastic Differential Equations With Non-globally Lipschitz Continuous Coefficients*, vol. 236. Providence, Rhodes Island: American Mathematical Society.
- JENTZEN, A. (2009) Pathwise numerical approximation of SPDEs with additive noise under non-global Lipschitz coefficients. *Potential Anal.*, **31**, 375–404.
- JENTZEN, A. (2010) Taylor expansions of solutions of stochastic partial differential equations. *Discrete Contin. Dyn. Syst. Ser. B*, **14**, 515–557.
- JENTZEN, A. & KLOEDEN, P. E. (2009) Overcoming the order barrier in the numerical approximation of stochastic partial differential equations with additive space-time noise. *Proc. R. Soc. Lond. Ser. A Math. Phys. Eng. Sci.*, **465**, 649–667.
- JENTZEN, A. & RÖCKNER, M. (2015) A Milstein scheme for SPDEs. *Foundations Comput. Math.*, **15**, 313–362.
- JIMENEZ, J., SHOJI, I. & OZAKI, T. (1999) Simulation of stochastic differential equations through the local linearization method: a comparative study. *J. Stat. Phys.*, **94**, 587–602.
- JIMENEZ, J. C. & CARBONELL, F. (2015) Convergence rate of weak local linearization schemes for stochastic differential equations with additive noise. *J. Comput. Appl. Math.*, **279**, 106–122.
- KLOEDEN, P. E., LORD, G. J., NEUENKIRCH, A. & SHARDLOW, T. (2011) The exponential integrator scheme for stochastic partial differential equations: pathwise error bounds. *J. Comput. Appl. Math.*, **235**, 1245–1260.
- KLOEDEN, P. & PLATEN, E. (2011) *Numerical Solution of Stochastic Differential Equations*. Stochastic Modelling and Applied Probability. Berlin: Springer Berlin Heidelberg.
- KOMORI, Y. & BURRAGE, K. (2014) A stochastic exponential Euler scheme for simulation of stiff biochemical reaction systems. *BIT*, **54**, 1067–1085.
- LI, X., JIANG, D. & MAO, X. (2009) Population dynamical behavior of Lotka–Volterra system under regime switching. *J. Comput. Appl. Math.*, **232**, 427–448.
- LORD, G. J., POWELL, C. E. & SHARDLOW, T. (2014) *An Introduction to Computational Stochastic PDEs*. New York: Cambridge University Press.
- LORD, G. J. & ROUGEMONT, J. (2004) A numerical scheme for stochastic PDEs with Gevrey regularity. *IMA J. Numer. Anal.*, **24**, 587–604.
- LORD, G. J. & TAMBUE, A. (2012) Stochastic exponential integrators for the finite element discretization of SPDEs for multiplicative and additive noise. *IMA J. Numer. Anal.*, **33**, 515–543.

- MAO, X. (1997) Stochastic differential equations and their applications. *Horwood Publishing Series in Mathematics & Applications*. Chichester: Horwood Publishing Limited, pp. xii+366.
- MORA, C. M. (2005) Weak exponential schemes for stochastic differential equations with additive noise. *IMA J. Numer. Anal.*, **25**, 486–506.
- ØKSENDAL, B. (2003) Stochastic differential equations. *Stochastic Differential Equations*. Berlin: Springer, pp. 65–84.
- PONS, O. (2016) *Inequalities in Analysis and Probability*. London: World Scientific.
- SAITO, Y. & MITSUI, T. (1996) Stability analysis of numerical schemes for stochastic differential equations. *SIAM J. Numer. Anal.*, **33**, 2254–2267.